MolTC: Towards Molecular Relational Modeling In Language Models

Junfeng Fang and Shuai Zhang and Chang Wu Zhiyuan Liu and Sihang Li and Kun Wang Wenjie Du and Xiang Wang and Xiangnan He

Abstract

Molecular Relational Learning (MRL), aiming to understand interactions between molecular pairs, plays a pivotal role in advancing biochemical research. Recently, the adoption of large language models (LLMs), known for their vast knowledge repositories and advanced logical inference capabilities, has emerged as a promising way for efficient and effective MRL. Despite their potential, these methods predominantly rely on the textual data, thus not fully harnessing the wealth of structural information inherent in molecular graphs. Moreover, the absence of a unified framework exacerbates the information underutilization, as it hinders the sharing of interaction rationale learned across diverse datasets. To address these challenges, this work proposes a novel LLM-based multimodal framework for Molecular in Teraction prediction following Chain-of-Thought (CoT) theory, termed MoITC, which can efficiently integrate rich graphical information of molecular pairs. For achieving a unified MRL, MolTC innovatively develops a dynamic parametersharing strategy for cross-dataset information exchange, and introduces a Multi-hierarchical CoT principle to refine training paradigm. Our experiments, conducted across twelve varied datasets involving over 4,000,000 molecular pairs, demonstrate the superiority of our method over current GNN and LLM-based baselines. On the top of that, a comprehensive Molecular Interactive Instructions dataset is constructed for the development of biochemical LLM, including our MolTC. Code is available at https://github.com/MangoKiller/MolTC.

1 Introduction

Molecular Relational Learning (MRL) (Lee et al., 2023a; Rozemberczki et al., 2022), aiming to understand interactions between molecular *pairs*, has gained significant interest due to its wide range of applications (Roden et al., 2020). For example, Drug-Drug Interactions (DDIs) are critical in pharmacology and drug development (Lin et al., 2020;

Deng et al., 2020), while solute-solvent interactions (SSIs) are fundamental in solution chemistry and the design of chemical processes (Varghese and Mushrif, 2019; Chung et al., 2022). However, the exhaustive experimental validation of these interactions is notoriously time-consuming and costly. In response, adopting large language models (LLMs) (Brown et al., 2020; Taylor et al., 2022), known for their vast knowledge repositories and advanced logical inference capabilities, has emerged as an efficient and effective alternative for MRL (Park et al., 2022; Jha et al., 2022a; Li et al., 2023b).

Despite their promise, a primary concern of current LLM-based paradigm is the insufficient data exploitation. Specifically, they predominantly rely on the textual data such as SMILES (Simplified Molecular Input Line Entry System) and property descriptions, thus not fully harnessing the wealth of structural information inherent in molecular graphs (Sagawa and Kojima, 2023; Chen et al., 2023), as indicated in Figure 1 (a). Recognizing the limitations of LLMs in comprehensive understanding complex graph structures through textual data alone, it's crucial to explicitly model these structures given their significance and complexity in MRL (Park et al., 2022).

Compounding this concern is the absence of a unified framework for LLM-based MRL (Livne et al., 2023; Pei et al., 2023). This gap impedes the efficient sharing and integration of interaction mechanisms learned from various datasets, leading to a fragmentation in knowledge and collective insights. Especially, it poses a catastrophic challenge for tasks with a limited number of labeled pairs (Varghese and Mushrif, 2019), which LLMs often struggle with due to the high risk of overfitting, as illustrated in Figure 1 (b). Worse still, such tasks are prevalent in MRL, where the experimental acquisition is often constrained by high costs and time-consuming processes (Lee et al., 2023a).

To overcome these limitations, in this work, we

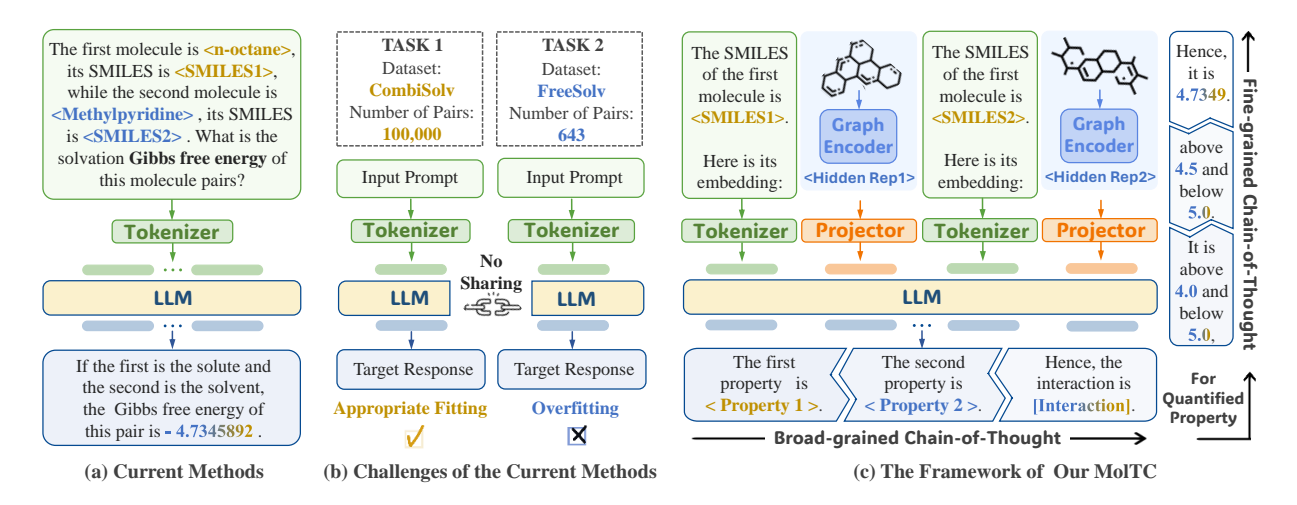


Figure 1: Comparison between the current methods leveraging LLMs to model molecule interactions and our MolTC. (a) The prevailing paradigm of current methods. (b) The challenge of applying the current paradigm to the tasks involving datasets with a small number of samples. (c) The framework of our proposed MolTC, which is enhanced by the principle of CoT. Best viewed in color.

propose MolTC, a unified LLM-based multi-modal framework for **Mol**ecular in**T**eraction prediction, enhanced by the CoT theory. As depicted in Figure 1 (c), MolTC employs the Graph Neural Networks (GNNs) (Kipf and Welling, 2017), known for their proficiency in graph modeling, to explicitly gather graphical information of molecular pairs, and encodes them into the input space of LLMs by two meticulously crafted projectors. In response to empirical findings that LLMs may confuse in differentiating the properties of two molecules in pairs, MolTC incorporates the molecules' SMILES information to reinforce the concept of molecular order. More importantly, to achieve a unified MRL, MolTC develops a Dynamic Parameter-sharing strategy for bolstering cross-dataset information exchange, which attributes to a dual win in efficiency and effectiveness.

On the top of that, a two-pronged approach is developed to foster this unified framework:

Training Paradigm Refinement: As shown in Figure 1 (c), we introduce a Multi-hierarchical CoT principle to enhance our MolTC. Specifically, the broad-grained CoT guides the pre-training phase to identify individual properties before predicting interactions, ensuring an acute awareness of the unique attributes each molecule brings to an interaction. For more challenging quantitative tasks where LLMs typically exhibit limitations, a fine-grained CoT enables the fine-tuning stage to initially predict a range for numerical interactive properties, then progressively refining it to a precise value.

Dataset Foundation Construction: As the preparation for above training paradigm, we conduct an extensive survey of various authoritative biochemical databases, and meticulously compile textual descriptions of molecules in diverse MRL dataset. Based on this, we construct a comprehensive dataset for **Mol**ecular InTeraction Instructions, termed **MoT-instruction**, for endowing current biochemical LLMs, including our MolTC, with enhanced MRL performance.

Our contributions can be summarized as follows:

- We identify the issue of insufficient data utilization in current LLM-based MRL methods, and take the first attempt to develop a unified LLMbased multi-modal framework, named MolTC.
- We introduce the multi-hierarchical CoT principle, which endows MolTC with efficient and effective interaction modeling capabilities, especially for challenging quantitative task.
- We construct MoT-instructions, the first comprehensive molecular interaction dataset for endowing current biochemical LLMs, including our MolTC, with enhanced MRL performance.
- Our experiments demonstrate the superiority of our method over current GNN and LLMbased baselines conducted across over 4,000,000 molecular pairs in various domain such as DDI, SSI and chromophore-solvent interaction (CSI).

2 Methodology

In this section, we detail our MolTC, which harnesses the power of LLMs for comprehending molecular interactions. We begin with the introduction of model framework in Section 2.1. Taking a step further, the training paradigm guided by the principle of Multi-hierarchical CoT is outlined in Section 2.2. Moreover, the dynamic parameter sharing strategy tailored for MolTC and our developed datasets, MoT-instructions, are elaborated in Section 2.3 and 2.4, respectively.

2.1 Framework of MolTC

Here we introduce four key components of MolTC's framework: Graph Encoder, Representation Projector, SIMLES Injector and the backbone LLM. The specific instantiation details of each module can be found in the experimental section.

Graph Encoder. The first step of extracting interactions is to precisely encode the molecular graphs. In sight of this, we utilize two GNN-based encoders to capture the embedding of the given molecular pairs, leveraging the GNN's robust capability in aggregating structural information. More formally, let $\mathcal{G}_a = \{\mathcal{V}_a, \mathcal{E}_a\}$ and $\mathcal{G}_b = \{\mathcal{V}_b, \mathcal{E}_b\}$ denote the input pair, where \mathcal{V}, \mathcal{E} represent atomic nodes and the chemical bonds, respectively. The two graph encoders f_{enc1} and f_{enc2} perform aggregating to obtain the atomic embedding:

$$\begin{aligned} \mathbf{H}_{a} &= [\boldsymbol{h}_{a}^{1}, \boldsymbol{h}_{a}^{2}, \dots, \boldsymbol{h}_{a}^{|\mathcal{V}_{a}|}] = f_{\mathsf{enc1}}(\mathcal{G}_{a}), \\ \mathbf{H}_{b} &= [\boldsymbol{h}_{b}^{1}, \boldsymbol{h}_{b}^{2}, \dots, \boldsymbol{h}_{b}^{|\mathcal{V}_{b}|}] = f_{\mathsf{enc2}}(\mathcal{G}_{b}), \end{aligned} \tag{1}$$

where h_a^i and h_b^i denote to the embedding of the *i*-th atom in molecule \mathcal{G}_a and \mathcal{G}_b ; \mathcal{V}_a and \mathcal{V}_b represent the number of nodes.

Representation Projector. After acquiring molecular pair representations \mathbf{H}_a and \mathbf{H}_b , the next step is to map them into the backbone LLM's hidden space using Projectors f_{pro1} and f_{pro2} . These projectors serve as pivotal connectors, translating \mathbf{H}_a and \mathbf{H}_b into LLM-comprehensible encodings \mathbf{M}_a and \mathbf{M}_b . Drawing inspiration from the state-of-theart vision-language models, we instantiate f_{pro1} and f_{pro2} by Querying Transformers (Q-Formers) (Li et al., 2023a; Dai et al.). More formally,

$$\mathbf{M}_{a} = [\boldsymbol{m}_{a}^{1}, \boldsymbol{m}_{a}^{2}, \dots, \boldsymbol{m}_{a}^{q}] = f_{\mathsf{pro1}}(\mathbf{H}_{a}),$$

$$\mathbf{M}_{b} = [\boldsymbol{m}_{b}^{1}, \boldsymbol{m}_{b}^{2}, \dots, \boldsymbol{m}_{b}^{q}] = f_{\mathsf{pro2}}(\mathbf{H}_{b}),$$
(2)

where q denotes the number of learnable query tokens of Q-Former's transformer.

In detail, our Projectors, based on the BERT architecture, incorporate an additional cross-attention module positioned between the self-attention and feed-forward modules. This instantiation offers two key benefits. Firstly, it supports seamless integration with conventional BERT-based text encoders, allowing f_{pro1} and f_{pro2} pre-training with extensive molecular graph-text pairs. Secondly, it maintains compatibility with various input dimensions d, and allows adjustments in the size of learnable query tokens to align with the LLM's token embedding size. These advantages lay a solid foundation for the thorough interaction of two molecules during the LLM's inference process. Future work will also explore more projector designs, such as streamlining it through specially tailored MLPs (Yang et al., 2023).

SMILES Tokenization. When directly analyzing the representations \mathbf{M}_a and \mathbf{M}_b with LLMs, our experiments suggest a potential confusion by LLMs in distinguishing the properties of each molecule in a pair. This observation naturally inspires us to integrate textual information of the molecules to strengthen the concept of their sequential order. Here MolTC employs SMILES due to its ubiquity and specificity. Additionally, SMILES serves as a conduit, linking the task-specific prompts with the corresponding biochemical knowledge stored within the LLM. Therefore, we directly input the SMILES of both molecules into the backbone LLM, utilizing the inherent encoder to acquire their tokens \mathbf{S}_a and \mathbf{S}_b .

Backbone LLM. MolTC leverages Galactica, a decoder-only transformer built on the OPT framework, as its backbone LLM. Pretrained on an extensive collection of scientific literature, Galactica demonstrates exceptional proficiency in biochemistry knowledge. This expertise, particularly in parsing molecular sequences such as SMILES and SELFIES strings, enables Galactica to adeptly capture the properties crucial for molecular interactions. Specifically, the goal of MolTC is to harness Galactica's advanced inferential skills to interpret the contextual interactions between two molecular sets of token collections, $\{M_a, S_a\}$ and $\{M_b, S_b\}$. More formally, we denote an integrated prompt

sequence as follows:

$$\mathbf{X} = \{\mathbf{P}, \mathbf{M}_a, \mathbf{S}_a, \mathbf{M}_b, \mathbf{S}_b\} = [\mathbf{x}_1, \mathbf{x}_2, ..., \mathbf{x}_l]$$

s.t. $\mathbf{P} \sim \mathcal{P}_{\mathbf{r}}$, (3)

where l is the integrated input length, \mathbf{P} denotes the task-specific prompt, and $\mathcal{P}_{\mathbf{r}}$ represents a collection of various manually designed prompts, each tailored for the molecular interaction task \mathbf{r} . The generation process adopts a causal mask to generate a response encapsulating key interactive properties with length T:

$$\hat{\mathbf{X}} = [\hat{x}_1, \hat{x}_2, ..., \hat{x}_T].$$
 (4)

Utilizing Galactica's autoregressive framework, the training objective involves regressing the target response based on the input prompt X. Specifically, the output for i-th token \hat{x}_i , is computed based on its preceding tokens as follows for $t \in (1,T)$:

$$p\left(\hat{\mathbf{X}}_{[1:t]}|\mathbf{X}\right) = \prod_{i=1}^{t} p\left(\hat{x}_i|\mathbf{X}, \hat{\mathbf{X}}_{[1:i-1]}\right). \quad (5)$$

2.2 Training Paradigm of MolTC

In this part, we elaborate the training paradigm of MolTC, including pretraining and fine-tuning processes, which is guided by the principle of Multihierarchical CoT, as shown in Figure 2.

2.2.1 Broad-grained CoT Guided Pretraining

Given the challenge of directly generating complex interactions from molecular pair data, the broad-grained CoT guides MoITC to initially identifying individual molecular properties. By thoroughly understanding each molecule's characteristics, MoITC establishes a solid foundation for accurately predicting their interactions. Specifically, in pretraining stage, the prompt is uniformly designed as follows:

Prompt for I	Pretraining Stage
Input Prompt	<smiles1>, <graemb1>, the front is the first molecule, followed by the second molecule: <smiles2>. <graemb2>. Please provide the biochemical properties of the two molecules one by one.</graemb2></smiles2></graemb1></smiles1>
Target Response	The properties of the first molecule are [Property1], and the properties of the second molecule are [Property2].

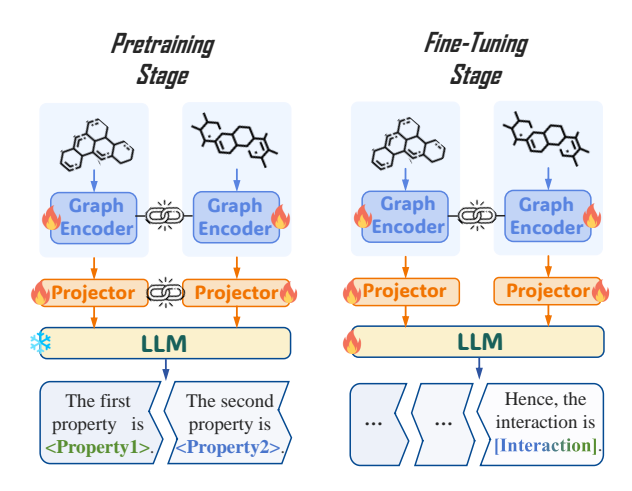


Figure 2: The training process of our proposed MolTC. Note that the flame denotes parameter updates occur; the snowflake indicates parameter updates are not performed; the chain link is utilized to depict parameter sharing between two modules. Best viewed in color.

This prompt design enable MoITC to delineate key properties of two molecules sequentially. Based on it, MoITC utilize the generation loss of the backbone LLM to train Graph Encoders, f_{enc1} and f_{enc2} , as well as the Representation Projectors, f_{pro1} and f_{pro2} . Notably, during this phase, the backbone LLM remains frozen.

Dataset Construction for Pretraining. To ensure backbone LLM can understands the individual characteristics of each molecule, it is pivotal to prepare a comprehensive dataset comprising molecule pairs and their corresponding biochemical properties. To this end, (1) we first conduct an extensive survey of various authoritative biochemical database such as Drugbank and PubChem (Kim et al., 2023), and collect a large amount of molecule-textual properties pairs; (2) then, recognizing the variability in annotation quality within this dataset, we augment and enrich molecular descriptions that were less extensively annotated; (3) subsequently, to simulate diverse molecular interactions, we generated molecular pairs by randomly grouping two distinct molecules from the above database. This random pairing facilitates a broad spectrum of molecular combinations, exposing the pretraining stage to diverse interaction scenarios, thus naturally enhances the generalizability of our MolTC.

2.2.2 Fine-grained CoT Guided Fine-tuning

During the fine-tuning phase, MolTC is trained to enable the backbone LLM to generate interaction properties based on the properties of individual molecules it initially identifies. To this end, prompts in fine-tuning stage should be crafted tailored to specific downstream task. For example, in DDI tasks, we construct the following prompt:

Prompt for DDI Tasks (Fine-tuning)							
Input Prompt	<smiles1>, <graemb1>, the front is the first molecule, followed by the second molecule: <smiles2>. <graemb2>. What are the side effects of these two drugs?</graemb2></smiles2></graemb1></smiles1>						
Target Response	The property of the first molecule is [Property1], while the property of the second molecule is [Property2]. Hence, the first drug molecule may increase the photosensitizing activities of the second drug molecule.						

Despite the effectiveness of this prompt design, LLMs face notable challenges in quantitative analysis, especially in complex molecular interaction contexts such as SSI and CSI. Our experiments in Section 3 highlight this difficulty, demonstrating that LLMs tend to exhibit indecision regarding the quantitative values in their outputs. To address this, a fine-graind CoT concept is introduced to refine the train paradigm. Specifically, the backbone LLM is guided to initially suggest a range for the target numerical value, then progressively refining it to a precise value. Take a meticulously prompt for SSI tasks as an example:

Prompt for S	SSI Tasks (Fine-tuning)
Input Prompt	<smiles1>, <graemb1>, the front is the first molecule, followed by the second molecule: <smiles2>.<graemb2>. What is the solvation Gibbs free energy of this pair of molecules?</graemb2></smiles2></graemb1></smiles1>
Target Response	The property of the first molecule is [Property1], while the property of the second molecule is [Property2]. Hence, the solvation Gibbs free energy of these two molecules is above 3.0 and below 3.5, so the accurate value is 3.24791.

This step-wise refinement process fosters a more accurate and reliable resolution of numerically-intensive challenges. Based on these prompts, in fine-tuning stage, the parameters in backbone LLM are updated through Low-Rank Adaptation (LoRA) (Hu et al., 2021) strategy, known for its efficiency in tailoring the LLM to the requirements of downstream tasks and minimal memory demands in storing gradients. Meanwhile, to ensures that other modules are optimally adjusted to suit the specifics of the downstream tasks, Graph Encoders f_{enc1} and f_{enc2} , as well as Representation Projectors f_{pro1} and f_{pro2} are trained following the generation loss of the backbone LLM.

2.3 Dynamic Parameter Sharing Strategy

To implement the above training paradigm effectively, we introduce a novel parameter sharing strategy, inspired by key biochemical insights:

- (1) The Importance of **Role-Playing**: A molecule's role in an interaction crucially influences the outcome. For example, in SSI scenario like the waterethanol pair, utilizing water and ethanol as solvents, respectively, yields different energy releases (Reichardt, 2021). Sometimes, a reversal of roles can even result in the absence of interaction.
- (2) The Importance of **Input Order**: In certain molecular pairs, the sequence of introducing molecules significantly impacts the interactions. For instance, the order of drug introduction can lead to varying therapeutic effects.
- (3) The Importance of **Role and Order-Specific** Feature Extraction: The role and input order of molecules determine the relevance of their structural features. For example, a chemical group in a solute-solvent pair may be crucial for the release of Gibbs free energy when in the solute, but less so in the solvent (Reichardt, 2021; J et al., 2022).

These insights inspire MolTC to adaptively prioritize distinct key information, creating unique tokens for the same molecule based on its role and order. To enable this nuanced learning while also capitalizing on the shared aspects of molecular learning, we introduce the following parameter sharing strategy, as shown in Figure 2:

- (1) The GNN-based **Encoders** f_{enc1} and f_{enc2} , which focus on extracting molecular graph structures, share parameters during both pretraining and fine-tuning stages to enhance learning efficiency.
- (2) The Qformer-based **Projectors** f_{pro1} and f_{pro2} ,

tasked with aligning molecular structures to semantic information, share parameters during pretraining stage to promote generalization and robustness. However, in the fine-tuning stage, we cease sharing to allow customized semantic mappings tailored to the varying roles and orders.

In summary, this strategy is tailored to balance the need for role and order-based distinctively learning with the efficiency gained from commonalities across molecular pairs.

2.4 Construction of MoT-instructions

Given the absence of a comprehensive instruction datasets tailored for LLM-based MRL, we aims to develop a molecular interactive instructions dataset, termed MoT-instructions. This dataset is designed to fulfill several key criteria: (1) it should include extensive molecular pairs capable of interaction, covering a broad spectrum of domains, (2) it should detail important biochemical properties of each molecule within these pairs, and (3) it should elaborate the resultant properties from molecular interactions. Specifically, MoT-instructions is constructed through a three-step process as follows.

- (1) We begin by aggregating twelve representative molecular interaction datasets across various widely recognized biochemical tasks, such as DDI, SSI and CSI. Following this, we engage in a systematic search for textual descriptions of the biochemical properties of each molecule involved in these interactions. Specifically, we source this information from authoritative biochemical databases such as DrugBank and PubChem.
- (2) The next critical step is the **experimental de**termination of the optimal instructions. Specifically, for all molecular pairs in step (1), we first deconstruct the lengthy molecular properties into a series of questions and answers, a format more comprehensible to LLMs (Taylor et al., 2022). The granularity of this deconstruction is decided based on the performance of our MolTC. For more challenge quantitative tasks, instructions guided by finegrained CoT are required to provide a numerical range before specifying a concrete value. Given the vast number of possible correct ranges, exhaustive testing is impractical. Therefore, we initially determine the optimal range for a small subset of datasets using grid search, guided by the predictive performance of MolTC. Subsequently, we derive statistics, such as mean and standard deviation, from these datasets to establish a relationship be-

tween statistics and optimal ranges. Finally, for other datasets, we determine their optimal range based on this established rule.

(3) The final step in our dataset construction involved filtering out pairs that lacked sufficient information on molecule properties or interaction data. Specifically, partial properties of a molecular pair are often missing in some datasets. To maximize the utilization of information from these datasets, we consider extracting each property within them as a separate dataset. This approach allows us to naturally omit missing values without wasting other information present in the molecular pair.

3 Experiment

In this section, we aim to answer the following research questions:

- **RQ1:** Is MoITC capable of generating the interactive property, involving the *qualitative* knowledge, of the given molecular pair?
- **RQ2:** Does MoITC have the ability to generate the interactive property, involving the *quantitative* property, for a given molecular pair?
- RQ3: What is the impact of the proposed strategies, such as the CoT enhancement strategy and SMILES injection strategy, on the inference process of our MolTC?

3.1 Experimental Setting

We evaluate MoITC on several well-established downstream molecule interaction tasks involving qualitative and quantitative analysis. Here we provide a brief overview of our experimental setup.

Datasets. We employ 12 datasets involving over 4,000,000 molecular pairs across various domain such as DDI, SSI and CSI. Specifically, we collect *Drugbank* (Version 5.0.3), *ZhangDDI* (Zhang et al., 2017), *ChChMiner* (Zitnik et al., 2018), *DeepDDI* (Ryu et al., 2018), *TWOSIDES* (Tatonetti et al., 2012), *Chromophore* (Joung et al., 2020), *MNSol* (Marenich et al., 2020), *FreeSolv* (Mobley and Guthrie, 2014), *CompSol* (Moine et al., 2017), *Abraham* (Grubbs et al., 2010), *CombiSolv* (Vermeire and Green, 2021) and *CombiSolv-QM* (Vermeire and Green, 2021).

Baselines. For a comprehensive evaluation, we conduct various baseline methods encompassing

Table 1: Comparative performance of various methods in qualitative interactive tasks. The best-performing methods are highlighted with a gray background, while the second-best methods are underscored for emphasis.

Baseline Model		_	bank AUC-ROC	6		Miner AUC-ROC	Deep	DDI AUC-ROC	
								. ,	
	GoGNN	$84.78_{\pm 0.57}$	$91.63_{\pm 0.66}$	$84.10_{\pm 0.46}$	$92.35_{\pm 0.48}$	$91.17_{\pm 0.46}$	$96.64_{\pm0.40}$	$93.54_{\pm 0.35}$	$92.71_{\pm 0.27}$
GNN	SSI-DDI	$94.12_{\pm 0.33}$	$98.38_{\pm0.31}$	$86.97_{\pm0.37}$	$93.76_{\pm0.34}$	$93.26_{\pm0.31}$	$97.81_{\pm 0.22}$	$95.27_{\pm 0.25}$	$98.42_{\pm0.31}$
Based	DSN-DDI	$94.93_{\pm 0.14}$	$99.01_{\pm 0.12}$	$87.65_{\pm0.13}$	$94.63_{\pm0.18}$	$84.30_{\pm0.17}$	$94.25_{\pm0.26}$	$95.64_{\pm0.18}$	$98.01_{\pm0.16}$
Dasca	CMRL	$94.83_{\pm0.12}$	$98.76_{\pm0.10}$	$87.78_{\pm 0.36}$	$94.68_{\pm 0.23}$	$94.23_{\pm 0.26}$	$98.37_{\pm0.12}$	$96.37_{\pm 0.34}$	$98.98_{\pm 0.31}$
	CGIB						$\underline{98.45}_{\pm0.31}$		
ML	DeepDDI	$93.15_{\pm 0.25}$	$98.06_{\pm 0.54}$	$83.35_{\pm0.49}$	$91.13_{\pm 0.58}$	$90.34_{\pm0.62}$	$95.73_{\pm0.37}$	$92.39_{\pm 0.38}$	$98.11_{\pm 0.42}$
Based MHCADD	MHCADDI	$78.50_{\pm0.80}$	$86.33_{\pm0.35}$	$77.86_{\pm0.59}$	$86.94_{\pm0.68}$	$84.26_{\pm0.54}$	$89.33_{\pm0.82}$	$87.01_{\pm 0.77}$	$88.64_{\pm0.83}$
	MDF-SA-DDI	$93.86_{\pm0.31}$	$97.65 {\scriptstyle \pm 0.29}$	$86.89_{\pm0.25}$	$94.03{\scriptstyle \pm 0.23}$	$93.64_{\pm0.20}$	$98.10_{\pm 0.19}$	$95.12_{\pm 0.30}$	$97.84_{\pm0.36}$
LLM Based	Galactica	$79.16_{\pm 0.35}$	$86.23_{\pm0.33}$	$67.20_{\pm0.46}$	$78.74_{\pm0.58}$	$74.61_{\pm 0.44}$	$83.51_{\pm0.63}$	$71.50_{\pm0.41}$	$79.07_{\pm0.41}$
	Chem T5	$85.83_{\pm0.31}$	$91.97_{\pm0.38}$	$72.34_{\pm0.42}$	$89.31_{\pm0.30}$	$80.79_{\pm 0.52}$	$85.65_{\pm0.46}$	$75.58_{\pm0.66}$	$84.42_{\pm0.43}$
	MolCA	$87.95_{\pm 0.52}$	$94.00_{\pm 0.37}$	$68.21_{\pm 0.59}$	$88.53_{\pm0.62}$	$90.15_{\pm0.43}$	$92.92_{\pm 0.60}$	$82.95_{\pm 0.58}$	$88.52_{\pm0.77}$
	MolT5						$91.18_{\pm 0.32}$		
Mo	lTC (Ours)	$95.98_{\pm0.15}$	$99.12_{\pm 0.31}$	$88.10_{\pm0.14}$	$94.86_{\pm0.17}$	$94.77_{\pm 0.23}$	$98.47_{\pm0.14}$	$96.70_{\pm0.26}$	$99.05_{\pm0.32}$

Table 2: Comparative performance of various methods in quantitative interactive tasks. The best-performing methods are highlighted with a gray background, while the second-best methods are underscored for emphasis.

Baseline Model	CombiS MAE	Solv-QM RMSE	Abra MAE	aham RMSE	Com MAE	pSol RMSE	Comb MAE	oiSolv RMSE
CIGIN GNN D-MPNN Based GEM CGIB	$0.470_{\pm 0.003} \\ 0.273_{\pm 0.002}$	$\begin{array}{c} 0.715_{\pm 0.004} \\ 0.596_{\pm 0.003} \end{array}$	$\begin{array}{c} 0.484_{\pm 0.004} \\ 0.264_{\pm 0.004} \end{array}$	$\begin{array}{c} 0.607_{\pm 0.006} \\ 0.705_{\pm 0.005} \\ 0.551_{\pm 0.005} \\ \underline{0.547}_{\pm 0.004} \end{array}$	$0.205_{\pm 0.006} \\ 0.203_{\pm 0.006}$	$0.373_{\pm 0.007} \\ 0.337_{\pm 0.007}$	$0.482_{\pm 0.003} \\ 0.290_{\pm 0.006}$	$\begin{array}{c} 0.895_{\pm 0.005} \\ 0.783_{\pm 0.009} \end{array}$
		$\begin{array}{c} 0.533_{\pm 0.005} \\ 0.587_{\pm 0.006} \end{array}$	$0.496_{\pm 0.006} \\ 0.355_{\pm 0.007}$	$0.693_{\pm0.006}$	$0.192_{\pm 0.008} \\ 0.198_{\pm 0.002}$	$0.353_{\pm 0.008} \\ 0.344_{\pm 0.003}$	$0.418_{\pm 0.007} \\ 0.267_{\pm 0.004}$	$\begin{array}{c} 0.711_{\pm 0.004} \\ 0.669_{\pm 0.005} \end{array}$
Galactica LLM Chem T5 Based MolCA MolT5	$0.463_{\pm 0.005}$	$\begin{array}{c} 0.895 _{\pm 0.007} \\ 0.785 _{\pm 0.006} \end{array}$	$0.629_{\pm 0.006} \\ 0.581_{\pm 0.007}$		$0.445_{\pm 0.008} \\ 0.467_{\pm 0.006}$	$\begin{array}{c} 0.734_{\pm 0.009} \\ 0.716_{\pm 0.005} \end{array}$	$0.882_{\pm 0.007} \\ 0.648_{\pm 0.006}$	$\begin{array}{c} 1.297_{\pm 0.007} \\ 1.125_{\pm 0.007} \end{array}$
MolTC (Ours)	$0.231_{\pm 0.002}$	$0.517_{\pm 0.003}$	$0.260_{\pm 0.004}$	$0.536_{\pm 0.005}$	$0.172_{\pm 0.006}$	$0.295_{\pm 0.004}$	$0.238_{\pm 0.003}$	$0.550_{\pm 0.004}$

distinct categories such as methods based on: GNNs, DL models other than GNN, and LLMs. Specifically, For DDI task, we employ GoGNN (Wang et al., 2020), MHCADDI (Deac et al., 2019), DeepDDI (Ryu et al., 2018), SSI-DDI, CGIB (Lee et al., 2023a), CMRL (Lee et al., 2023b), MDF-SA-DDI (Lin et al., 2022), DSN-DDI (Li et al., 2023c) as the backbone. For SSI and CSI tasks, we untilize D-MPNN (Vermeire and Green, 2021), SolvBert (Yu et al., 2023), SMD (Meng et al., 2023), CGIB (Lee et al., 2023a), CIGIN (Pathak et al., 2020), GEM (Fang et al., 2022), GOVER (Rong et al., 2020), Uni-Mol (Zhou et al., 2023) as the backbone. Furthermore, all downstream tasks adopt LLM-based methods, such as Galactica (Taylor et al., 2022), Chem T5 (Christofidellis et al., 2023), MolT5 (Edwards et al., 2022) and MolCA (Liu

et al., 2023), as the backbone.

Modules. In our experiments, the two graph encoder are instantiated by the five-layer GINE (Hu et al., 2019). We conduct 2 million molecules from the ZINC15 (Sterling and Irwin, 2015) dataset to pretrain them by contrastive learning following MolCA (Liu et al., 2023). Similarly, two projector are initialized with the encoder-only transformer, Sci-BERT, which is pretrained on scientific publications (Beltagy et al., 2019), while its cross-attention modules are randomly initialized.

Metrics. For qualitative tasks, we employ prediction *Accuracy* and *AUC-ROC* (Area Under the Receiver Operating Characteristic curve) as comparative metrics, while for quantitative tasks, *MAE* (Mean Absolute Error) and *RMSE* (Root Mean

Table 3: Performance comparison of various models on different datasets.

Dataset	Metric	w/o SMILES	w/o CoT			
			Broad	Fine		
DDI	Accuracy Rate (\dagger)	$6.42_{\pm 0.13} \ 7.08 \%$	$\begin{array}{c c} 2.01_{\pm 0.05} \\ 2.13 \% \end{array}$	_ _		
	ACC-AUC Rate (↓)	$7.87_{\pm 0.32} \\ 8.22 \%$	$\begin{array}{c c} 2.98_{\pm 0.08} \\ 3.10 \ \% \end{array}$	_ _		
SSI	MAE Rate (†)	$0.025_{\pm 0.004}\atop11.32~\%$	$0.010_{\pm 0.002}\atop -4.56~\%$	$0.036 \scriptstyle{\pm 0.007} \\ 16.40 \%$		
	RMSE Rate (†)	$\begin{array}{c} 0.045_{\pm 0.007} \\ 9.47 \ \% \end{array}$	$0.014_{\pm 0.003}\atop 2.95~\%$	$0.054_{\pm 0.009}\atop11.37~\%$		
CSI Abs.	MAE Rate (†)	$2.06_{\pm 0.11}$ 15.03%	$0.51_{\pm 0.03} \\ 3.72 \%$	$2.65_{\pm 0.16}$ 19.34%		
	RMSE Rate (†)	$3.37_{\pm 0.20}$ 15.18%	$\begin{array}{c} 1.18_{\pm 0.12} \\ 5.31 \ \% \end{array}$	$4.84_{\pm 0.29}$ 21.80 %		
CSI Emis.	MAE Rate (†)	$3.10_{\pm 0.17} \\ 16.23 \%$	$0.85_{\pm 0.04} \\ 5.23 \%$	$4.42_{\pm 0.36}$ 23.14%		
	RMSE Rate (†)	$4.99_{\pm 0.28}$ 18.34%	${}^{1.47}_{\pm0.12}_{5.40\%}$	$7.29_{\pm 0.44}$ 26.80%		
CSI Life.	MAE Rate (†)	$0.085 \scriptstyle{\pm 0.003} \\ 13.70 \%$	$\begin{bmatrix} 0.026_{\pm 0.002} \\ 4.19 \% \end{bmatrix}$	$0.072 \scriptstyle{\pm 0.004} \\ 11.61 \%$		
	RMSE Rate (†)	$0.101_{\pm 0.010} \\ 12.16 \%$	$\begin{bmatrix} 0.034_{\pm 0.008} \\ 4.09 \% \end{bmatrix}$	$0.093_{\pm 0.010}\atop11.20~\%$		

Square Error) are utilized as the standards.

3.2 Qualitative Prediction Performance (RQ1)

Table 1 exhibits the performance in qualitative interactive tasks. Due to page width limitations, only a subset of the results is presented. Note that for LLM-based methods, we fine-tune the backbone LLMs on task-specific datasets for fair comparison. Their prediction is considered accurate only if the outputs include words or numbers that correctly depict the interaction in question, without presenting any that describe alternative interactions. From Table 1, we deduce the following observations:

- Obs. 1: MoITC consistently outshines its counterparts in qualitative interaction predictions. While GNN-based methods demonstrate commendable performance, maintaining over 90% accuracy across numerous datasets, MoITC transcends these figures in every evaluated scenario. For instance, it marks a notable 1.05% improvement in accuracy on the drugback dataset, a feat attributable to the synergy between the LLMs' sophisticated reasoning faculties and the GNNs' adept graph data interpretation.
- **Obs. 2:** The variability of MolTC's outcomes, as indicated by the standard deviation, is consis-

tently minimal in comparison to other models. On average, the standard deviation for MolTC is 35.41% lower than GNN-based models and 46.86% lower than LLM-based models. The precision in MolTC's performance is largely attributed to the training paradigm enhanced by the multi-hierarchical CoT, which ensures a meticulous and accurate inference process.

3.3 Quantitative Prediction Performance (RQ2)

Table 2 delineates the performance of various models in a subset of quantitative tasks. The datasets offer a four-dimensional molecular information, comprising atom type, chirality tag, bond type, and bond direction. Key observations from Table 2 include:

- Obs. 3: MoITC continues to lead in quantitative analysis tasks, an area typically challenging for LLMs. Despite the strong baseline set by CGIB, characterized by low MAE and RMSE across datasets, MoITC outperforms it in every metric. For instance, it achieves a 19.32% reduction in RMSE on the CombiSolv dataset relative to CGIB. This underscores the advantage of adeptly leveraging the interaction between SMILE representations and molecular graph structures.
- Obs. 4: LLM-based models, in general, exhibit subpar performance in quantitative tasks compared to traditional DL-based models. This is primarily attributed to their inadequacy in sharing and transferring learned molecular interaction insights across datasets during the fine-tuning phase and the absence of CoT-guided inference, underscoring the significance of a unified framework for molecular interaction predictions.

3.4 Ablation Study (RQ3)

Table 3 presents an ablation study aimed at dissecting the influence of SMILE auxiliary analysis and the optimized training paradigms based on Broad-grained and Fine-grained CoT. For the CSI dataset, properties such as the maximum absorption wavelength (Absorption), maximum emission wavelength (Emission), and excited state lifetime (Lifetime) are denoted as Abs., Emis., and Life., respectively. Key observations are as follows:

• **Obs. 5:** The three studied ablations exhibit significant influence on the results. For example, the exclusion of SMILES results in an average

accuracy downturn of 13.76%, highlighting the critical role of integrating SMILES as delineated in Section 2.1. That is, injecting SMILES notably augments the LLM's receptiveness to molecular sequences, thereby elevating the accuracy of the outcomes. Meanwhile, the collective impact of these three ablations registers an average drop of 12.77%, affirming the substantial enhancement imparted by the proposed strategies to MoITC.

- **Obs. 6:** The most pronounced effect is observed with the ablation of the Fine-grained CoT training paradigm, which incurs an average accuracy decrement of 18.82%. This underscores the pivotal role of guiding the LLM to initially deduce a numerical range, a strategy particularly beneficial for quantitative analysis tasks, typically a challenging domain for LLMs.
- **Obs. 7:** The least pronounced, yet significant, impact stems from the optimization of the Broadgrained CoT training paradigm, with an average accuracy reduction of 4.35%. Its importance is particularly underscored for molecular pairs involving larger and more complex molecules, where directly predicting interactive property by LLMs is arduous.

4 Related Work

Since exhaustive experimental validation of the molecule interactions is notoriously time-consuming and costly (Lee et al., 2023a; Guo et al., 2023), more recently, adopting LLM has emerged as a promising alternative for efficient and effective molecular relational learning, which are known for their vast knowledge repositories and advanced logical inference capabilities. Specifically,

• (Park et al., 2022; Jha et al., 2022a,b) focus on employ LLM to optimize **protein-protein interactions** (**PPI**) tasks. In this context, proteins are represented as residue contact graphs, also known as amino acid graphs, where each node is a residue (Jha et al., 2022b). Notably, (Jha et al., 2022b) leverages the superior encoding capabilities of the biochemical LLMs, where the input to the LLM is the protein sequence, and the output is a feature vector for each amino acid in the sequence. This output is then used as node features in the residue contact graph to enhance the prediction of PPI tasks.

- (Sagawa and Kojima, 2023; Chen et al., 2023; Livne et al., 2023; Shi et al., 2023) focus using LLMs to optimize chemical reactions. Specifically, (Shi et al., 2023) selects in-context reaction examples with varying confidence scores closest to the target reaction query, encouraging large models to understand the relationships between these reactions. (Sagawa and Kojima, 2023) focuses on optimizing low-sample organic chemical applications by pretraining them with extensive compound libraries and fine-tuning with smaller in-house datasets for specific tasks. (Livne et al., 2023) introduces a new foundational model, nach0, capable of solving various chemical and biological tasks, including molecular synthesis.
- (Li et al., 2023b; Pei et al., 2023) focus on using LLMs to optimize tasks related to **drug molecules**. Specifically, (Pei et al., 2023) enriches cross-modal integration in biology with chemical knowledge and natural language associations, achieving significant results in multiple drug-target interaction prediction tasks. Meanwhile, (Li et al., 2023b) concentrates on few-shot drug pair synergy prediction.

5 Conclusion

This work focuses on molecule rationale learning, which plays a pivotal role in predicting molecular interactive properties. Specifically, we introduce a novel, unified LLM-based framework for predicting molecular interactive properties, termed MolTC. To efficiently train it, we propose a multitiered CoT principle to guide the training paradigm. That is, a broad-grained CoT aims to guide the pretraining phase by sequentially identifying properties of individual molecules, and a fine-grained CoT caters to more challenging quantitative analysis tasks. Experiments, conducted across twelve varied datasets and involving over 4,000,000 molecular pairs, demonstrate the superiority of our method over current GNN and LLM-based baselines. This breakthrough sets a new standard for integrating multimodal data in LLM-based MRL.

Limitations

While this research has undergone extensive testing across a diverse array of datasets covering various domains, it does have certain limitations. Specifically, the study has not been subjected to datasets comprising exceptionally large or multiple molecules, which represent extreme cases. Furthermore, the methodologies employed in this research have not yet been adapted or evaluated in contexts requiring few-shot or zero-shot learning scenarios. Future endeavors will focus on expanding the scope of this study to encompass these areas.

References

- Iz Beltagy, Kyle Lo, and Arman Cohan. 2019. Scibert: A pretrained language model for scientific text. *arXiv* preprint arXiv:1903.10676.
- Tom Brown, Benjamin Mann, Nick Ryder, Melanie Subbiah, Jared D Kaplan, Prafulla Dhariwal, Arvind Neelakantan, Pranav Shyam, Girish Sastry, Amanda Askell, et al. 2020. Language models are few-shot learners. *Advances in neural information processing systems*, 33:1877–1901.
- Kexin Chen, Junyou Li, Kunyi Wang, Yuyang Du, Jiahui Yu, Jiamin Lu, Guangyong Chen, Lanqing Li, Jiezhong Qiu, Qun Fang, et al. 2023. Towards an automatic ai agent for reaction condition recommendation in chemical synthesis. *arXiv preprint arXiv:2311.10776*.
- Dimitrios Christofidellis, Giorgio Giannone, Jannis Born, Ole Winther, Teodoro Laino, and Matteo Manica. 2023. Unifying molecular and textual representations via multi-task language modelling. *arXiv* preprint arXiv:2301.12586.
- Yunsie Chung, Florence H Vermeire, Haoyang Wu, Pierre J Walker, Michael H Abraham, and William H Green. 2022. Group contribution and machine learning approaches to predict abraham solute parameters, solvation free energy, and solvation enthalpy. *Journal of Chemical Information and Modeling*, 62(3):433–446.
- W Dai, J Li, D Li, AMH Tiong, J Zhao, W Wang, B Li, P Fung, and S Hoi. Instructblip: Towards general-purpose vision-language models with instruction tuning. arxiv 2023. arXiv preprint arXiv:2305.06500.
- Andreea Deac, Yu-Hsiang Huang, Petar Veličković, Pietro Liò, and Jian Tang. 2019. Drug-drug adverse effect prediction with graph co-attention. *arXiv* preprint arXiv:1905.00534.
- Yifan Deng, Xinran Xu, Yang Qiu, Jingbo Xia, Wen Zhang, and Shichao Liu. 2020. A multimodal deep learning framework for predicting drug—drug interaction events. *Bioinformatics*, 36(15):4316–4322.
- Carl Edwards, Tuan Lai, Kevin Ros, Garrett Honke, Kyunghyun Cho, and Heng Ji. 2022. Translation between molecules and natural language. *arXiv* preprint arXiv:2204.11817.

- Xiaomin Fang, Lihang Liu, Jieqiong Lei, Donglong He, Shanzhuo Zhang, Jingbo Zhou, Fan Wang, Hua Wu, and Haifeng Wang. 2022. Geometry-enhanced molecular representation learning for property prediction. *Nature Machine Intelligence*, 4(2):127–134.
- Laura M Grubbs, Mariam Saifullah, E Nohelli, Shulin Ye, Sai S Achi, William E Acree Jr, and Michael H Abraham. 2010. Mathematical correlations for describing solute transfer into functionalized alkane solvents containing hydroxyl, ether, ester or ketone solvents. *Fluid phase equilibria*, 298(1):48–53.
- Taicheng Guo, Kehan Guo, Bozhao Nan, Zhenwen Liang, Zhichun Guo, Nitesh V Chawla, Olaf Wiest, and Xiangliang Zhang. 2023. What can large language models do in chemistry? a comprehensive benchmark on eight tasks. *arXiv preprint arXiv:2305.18365*.
- Edward J Hu, Yelong Shen, Phillip Wallis, Zeyuan Allen-Zhu, Yuanzhi Li, Shean Wang, Lu Wang, and Weizhu Chen. 2021. Lora: Low-rank adaptation of large language models. *arXiv preprint arXiv:2106.09685*.
- Weihua Hu, Bowen Liu, Joseph Gomes, Marinka Zitnik, Percy Liang, Vijay Pande, and Jure Leskovec. 2019. Strategies for pre-training graph neural networks. *arXiv preprint arXiv:1905.12265*.
- Burrows C J, Harper J B, and et al. Sander W. 2022. Solvation effects in organic chemistry. *The Journal of Organic Chemistry*, 87(3):1599–1601.
- Kanchan Jha, Sriparna Saha, and Hiteshi Singh. 2022a. Prediction of protein–protein interaction using graph neural networks. *Scientific Reports*, 12(1):8360.
- Kanchan Jha, Sriparna Saha, and Hiteshi Singh. 2022b. Prediction of protein–protein interaction using graph neural networks. *Scientific Reports*, 12(1):8360.
- Joonyoung F Joung, Minhi Han, Minseok Jeong, and Sungnam Park. 2020. Experimental database of optical properties of organic compounds. *Scientific data*, 7(1):295.
- Sunghwan Kim, Jie Chen, Tiejun Cheng, Asta Gindulyte, Jia He, Siqian He, Qingliang Li, Benjamin A. Shoemaker, Paul A. Thiessen, Bo Yu, Leonid Zaslavsky, Jian Zhang, and Evan E. Bolton. 2023. Pubchem 2023 update. *Nucleic Acids Res.*, 51(D1):1373–1380.
- Thomas N. Kipf and Max Welling. 2017. Semisupervised classification with graph convolutional networks. In *ICLR (Poster)*.
- Namkyeong Lee, Dongmin Hyun, Gyoung S. Na, Sungwon Kim, Junseok Lee, and Chanyoung Park. 2023a. Conditional graph information bottleneck for molecular relational learning. In *ICML*, volume 202 of *Proceedings of Machine Learning Research*, pages 18852–18871. PMLR.

- Namkyeong Lee, Kanghoon Yoon, Gyoung S Na, Sein Kim, and Chanyoung Park. 2023b. Shift-robust molecular relational learning with causal substructure. *arXiv preprint arXiv:2305.18451*.
- Junnan Li, Dongxu Li, Silvio Savarese, and Steven Hoi. 2023a. Blip-2: Bootstrapping language-image pretraining with frozen image encoders and large language models. arXiv preprint arXiv:2301.12597.
- Tianhao Li, Sandesh Shetty, Advaith Kamath, Ajay Jaiswal, Xiaoqian Jiang, Ying Ding, and Yejin Kim. 2023b. Cancergpt: Few-shot drug pair synergy prediction using large pre-trained language models. *ArXiv*.
- Zimeng Li, Shichao Zhu, Bin Shao, Xiangxiang Zeng, Tong Wang, and Tie-Yan Liu. 2023c. Dsn-ddi: an accurate and generalized framework for drug–drug interaction prediction by dual-view representation learning. *Briefings in Bioinformatics*, 24(1):bbac597.
- Shenggeng Lin, Yanjing Wang, Lingfeng Zhang, Yanyi Chu, Yatong Liu, Yitian Fang, Mingming Jiang, Qiankun Wang, Bowen Zhao, Yi Xiong, et al. 2022. Mdf-sa-ddi: predicting drug–drug interaction events based on multi-source drug fusion, multi-source feature fusion and transformer self-attention mechanism. *Briefings in Bioinformatics*, 23(1):bbab421.
- Xuan Lin, Zhe Quan, Zhi-Jie Wang, Tengfei Ma, and Xiangxiang Zeng. 2020. Kgnn: Knowledge graph neural network for drug-drug interaction prediction. In *IJCAI*, volume 380, pages 2739–2745.
- Zhiyuan Liu, Sihang Li, Yanchen Luo, Hao Fei, Yixin Cao, Kenji Kawaguchi, Xiang Wang, and Tat-Seng Chua. 2023. Molca: Molecular graph-language modeling with cross-modal projector and uni-modal adapter. *arXiv preprint arXiv:2310.12798*.
- Micha Livne, Zulfat Miftahutdinov, Elena Tutubalina, Maksim Kuznetsov, Daniil Polykovskiy, Annika Brundyn, Aastha Jhunjhunwala, Anthony Costa, Alex Aliper, and Alex Zhavoronkov. 2023. nach0: Multimodal natural and chemical languages foundation model. *arXiv preprint arXiv:2311.12410*.
- Aleksandr V Marenich, Casey P Kelly, Jason D Thompson, Gregory D Hawkins, Candee C Chambers, David J Giesen, Paul Winget, Christopher J Cramer, and Donald G Truhlar. 2020. Minnesota solvation database (mnsol) version 2012.
- Fanwang Meng, Hanwen Zhang, Juan Samuel Collins-Ramirez, and Paul W. Ayers. 2023. Something for nothing: Improved solvation free energy prediction with learning.
- David L Mobley and J Peter Guthrie. 2014. Freesolv: a database of experimental and calculated hydration free energies, with input files. *Journal of computer-aided molecular design*, 28:711–720.

- Edouard Moine, Romain Privat, Baptiste Sirjean, and Jean-Noël Jaubert. 2017. Estimation of solvation quantities from experimental thermodynamic data: Development of the comprehensive compsol databank for pure and mixed solutes. *Journal of Physical and Chemical Reference Data*, 46(3).
- Gilchan Park, Sean McCorkle, Carlos Soto, Ian Blaby, and Shinjae Yoo. 2022. Extracting protein-protein interactions (ppis) from biomedical literature using attention-based relational context information. In 2022 IEEE International Conference on Big Data (Big Data), pages 2052–2061. IEEE.
- Yashaswi Pathak, Siddhartha Laghuvarapu, Sarvesh Mehta, and U Deva Priyakumar. 2020. Chemically interpretable graph interaction network for prediction of pharmacokinetic properties of drug-like molecules. In *Proceedings of the AAAI Conference on Artificial Intelligence*, volume 34, pages 873–880.
- Qizhi Pei, Wei Zhang, Jinhua Zhu, Kehan Wu, Kaiyuan Gao, Lijun Wu, Yingce Xia, and Rui Yan. 2023. Biot5: Enriching cross-modal integration in biology with chemical knowledge and natural language associations. *arXiv* preprint arXiv:2310.07276.
- C. Reichardt. 2021. Solvation effects in organic chemistry: A short historical overview. *The Journal of Organic Chemistry*, 87(3):1616–1629.
- Dan M Roden, Robert A Harrington, Athena Poppas, and Andrea M Russo. 2020. Considerations for drug interactions on qtc in exploratory covid-19 treatment. *Circulation*, 141(24):e906–e907.
- Yu Rong, Yatao Bian, Tingyang Xu, Weiyang Xie, Ying Wei, Wenbing Huang, and Junzhou Huang. 2020. Self-supervised graph transformer on largescale molecular data. In *NeurIPS*.
- Benedek Rozemberczki, Stephen Bonner, Andriy Nikolov, Michaël Ughetto, Sebastian Nilsson, and Eliseo Papa. 2022. A unified view of relational deep learning for drug pair scoring. In *IJCAI*, pages 5564–5571. ijcai.org.
- Jae Yong Ryu, Hyun Uk Kim, and Sang Yup Lee. 2018. Deep learning improves prediction of drug–drug and drug–food interactions. *Proceedings of the national academy of sciences*, 115(18):E4304–E4311.
- Tatsuya Sagawa and Ryosuke Kojima. 2023. Reactiont5: a large-scale pre-trained model towards application of limited reaction data. *arXiv preprint arXiv:2311.06708*.
- Yaorui Shi, An Zhang, Enzhi Zhang, Zhiyuan Liu, and Xiang Wang. 2023. Relm: Leveraging language models for enhanced chemical reaction prediction. In *EMNLP (Findings)*, pages 5506–5520. Association for Computational Linguistics.
- Teague Sterling and John J Irwin. 2015. Zinc 15–ligand discovery for everyone. *Journal of chemical information and modeling*, 55(11):2324–2337.

- Nicholas P Tatonetti, Patrick P Ye, Roxana Daneshjou, and Russ B Altman. 2012. Data-driven prediction of drug effects and interactions. *Science translational medicine*, 4(125):125ra31–125ra31.
- Ross Taylor, Marcin Kardas, Guillem Cucurull, Thomas Scialom, Anthony Hartshorn, Elvis Saravia, Andrew Poulton, Viktor Kerkez, and Robert Stojnic. 2022. Galactica: A large language model for science. *arXiv* preprint arXiv:2211.09085.
- Jithin John Varghese and Samir H Mushrif. 2019. Origins of complex solvent effects on chemical reactivity and computational tools to investigate them: a review. *Reaction Chemistry & Engineering*, 4(2):165–206.
- Florence H Vermeire and William H Green. 2021. Transfer learning for solvation free energies: From quantum chemistry to experiments. *Chemical Engineering Journal*, 418:129307.
- Hanchen Wang, Defu Lian, Ying Zhang, Lu Qin, and Xuemin Lin. 2020. Gognn: Graph of graphs neural network for predicting structured entity interactions. *arXiv* preprint arXiv:2005.05537.
- Zhengyi Yang, Jiancan Wu, Yanchen Luo, Jizhi Zhang, Yancheng Yuan, An Zhang, Xiang Wang, and Xiangnan He. 2023. Large language model can interpret latent space of sequential recommender. *arXiv preprint arXiv:2310.20487*.
- Jiahui Yu, Chengwei Zhang, Yingying Cheng, Yun-Fang Yang, Yuan-Bin She, Fengfan Liu, Weike Su, and An Su. 2023. Solvbert for solvation free energy and solubility prediction: a demonstration of an nlp model for predicting the properties of molecular complexes. *Digital Discovery*, 2(2):409–421.
- Wen Zhang, Yanlin Chen, Feng Liu, Fei Luo, Gang Tian, and Xiaohong Li. 2017. Predicting potential drugdrug interactions by integrating chemical, biological, phenotypic and network data. *BMC bioinformatics*, 18:1–12.
- Gengmo Zhou, Zhifeng Gao, Qiankun Ding, Hang Zheng, Hongteng Xu, Zhewei Wei, Linfeng Zhang, and Guolin Ke. 2023. Uni-mol: a universal 3d molecular representation learning framework.
- M Zitnik, R Sosi, S Maheshwari, and J Leskovec. 2018. Stanford biomedical network dataset collection. *Biosn. Datasets Stanford Biomed. Netw. Dataset Collect.*